$P_{2S+1}(\{2S+1\})$ with indices, $\{2S+1\}$, contained in $g_i$ and $\prod'$ is the product over all other $(2S+1)$-tuples of indices. The leading term in the expansion of $\prod'$ in 1 and $I_{2S+1}$ is just unity. All further terms violate $P$. The full contribution of $P$ to (D1) is thus contained in $\prod_i H_{n_i}P_{n_i}$ and is simply given by $\prod_i \mathcal{C}(H_{n_i}P_{n_i})$. The contribution of any partition $P$ to (D1) may be obtained in this way, so (D3) holds. When the trace of (D3) is taken to evaluate $Q_n$ by (58), the equivalence in the trace of different distributions of the arguments $(1\cdots n)$ for fixed $m_l$ provides the numerical factors necessary to identify $b_l$ from (55). Equation (63) results.

The above argument is general enough to prove the structure (D3) for the full $H_n(1\cdots n;1'\cdots n')\times P_n(1'\cdots n')$. This is of some interest, since it allows (48) to be converted into an integral equation directly for $\mathcal{C}(H_nP_n)$. Note in passing that $\mathfrak{D}(H_nP_n)=\mathfrak{D}(D_nP_n)$, so (48) is certainly consistent with (D3).

PHYSICAL REVIEW VOLUME 138, NUMBER 4A 17 MAY 1965

# Superconducting and Normal State Properties of Dilute Indium-Tin Alloys: Bulk and Thin Film

A. M. TOXEN, M. J. BURNS,* AND D. J. QUINN†
*IBM Watson Research Center, Yorktown Heights, New York*
(Received 23 December 1964)

Measurements are reported of normal-state and superconducting-state properties of bulk and thin-film indium-tin alloys. For the bulk samples, whose compositions were in the range 0–5.8 at.% tin, the residual resistivities, critical magnetic fields, and critical temperatures were measured. It is shown that both similarity conditions are well obeyed for the critical fields of samples containing 0–1.8 at.% Sn, for which detailed data were taken. High-purity films were produced containing up to 5 at.% tin. From resistance measurements, the critical temperatures, critical fields, thicknesses, and residual resistivities of the films were obtained. The formula for boundary scattering due to Fuchs has been recast into a more convenient form from which one may calculate the intrinsic mean free path and intrinsic resistivity directly from the measured resistivity and thickness. From the resistivity measurements, one may infer a value for the product of intrinsic resistivity and mean free path, $\rho l$, of $1.6\times10^{-11}\ \Omega\,\text{cm}^2$. The critical-temperature measurements indicate that bulk and film specimens having the same composition do not have the same critical temperature. On the basis of a model which attributes the shift in critical temperature to stress effects, formulas are derived from which one may calculate the stress in a film as well as the equivalent (i.e., stress-shifted) bulk critical field for any film. However, the stress-shifted bulk critical-field curves obtained in this way for the indium alloy films are nearly the same as one would have obtained under the assumption of similarity. Analysis of the critical-temperature results indicates that while stresses in the most dilute films are probably relieved by ordinary dislocation flow, some other mechanism, perhaps twinning, dominates in the more concentrated alloys. The largest uniaxial stress calculated for the films studied was $2.6\times10^9$ dyn/cm², which was obtained for a film of indium containing 2.6 at.% tin.

## INTRODUCTION

WITH a view to studying and understanding mean-free-path effects upon the critical fields of superconducting alloy films, a study was undertaken of dilute alloys of indium containing tin. The indium-tin system was chosen for several reasons. First, the critical temperatures of the dilute alloys, i.e., 0–5 at.% Sn, lie in a temperature range which is convenient for measurement, 3.4–3.9°K. Second, both constituents have low boiling points, which makes for ease of evaporation. Third, since the self-diffusion of indium and the diffusion of tin in indium are both relatively large at room temperature, well-annealed, homogeneous alloy films are readily obtained. Finally, previous work on indium films[1] had demonstrated that their superconducting properties are well behaved and indicated that indium alloy films might also have well-behaved properties.

To properly analyze film critical-field data, one must know the critical fields of bulk samples having the same compositions as the films. For this reason, a careful study of bulk indium-tin alloys was also undertaken.

The work to be reported falls naturally into two parts: that related to measurements on the bulk specimens, and that pertaining to the evaporated films. Therefore, the paper will be divided into two sections.

In Part 1, measurements of the residual resistivity, critical temperature $T_c$, and critical field $H_c$ of the bulk alloys are reported. The composition range studied was 0–5.8 at.% tin in indium. The concept of similarity is discussed and it is shown that both similarity conditions are quite well obeyed for samples containing 0–1.8 at.% Sn, for which detailed data were taken.

In Part 2, the film measurements are discussed. The discussion includes the preparation of the films, their compositions, the electrical measurements made upon them, and their critical temperatures. From the electrical measurements, the intrinsic residual resistivity (corrected for boundary scattering) is obtained and together with the critical temperature measurements,

* Present address: IBM Components Division, East Fishkill, New York.
† Present address: United Aircraft Research Laboratory, East Hartford, Connecticut.
[1] A. M. Toxen, Phys. Rev. 123, 442 (1961).

is compared to the corresponding bulk measurements.

In earlier studies of the properties of pure indium films,[1,2] it was found that the critical temperatures of thin films were not quite the same as those of bulk samples and that the difference could be attributed to stresses in the films brought about by the differential contraction of film and substrate on being cooled below room temperature. Similar effects are found for the alloy films and a model is presented whereby the film stress is calculated from the critical temperature shift. From this model, the stress-shifted "bulk critical field" can then be calculated.

In previous publications, the thickness,[3] mean free path,[4] and temperature[5] dependence of the film critical fields have been analyzed. Hence these results will not be included.

## PART 1: BULK

### I. Sample Preparation

The series of alloys studied were prepared from high-purity Sn and In supplied by the Consolidated Mining and Smelting Company of Canada. The constituents, in quartz tubes, were melted in a vacuum of approximately $1\times10^{-6}$ Torr, sealed off, and mechanically mixed in rotating ovens for 20 min. A cold water quench was then employed to inhibit segregation. Samples were formed by extruding the alloys into 0.040-in. wires. Prior to measurement, the wires were again sealed into evacuated glass tubes and annealed at 125°C for two weeks.

### II. Experimental Equipment and Techniques

Resistances were determined from the slope of the current-voltage curves measured with a microvolt potentiometer.

Temperature was controlled by maintaining a constant vapor pressure above the He bath with a sensitive manostat. The samples were directly immersed in the liquid-He bath and a U-tube manometer and cathetometer were employed to measure the He vapor pressure. A solenoid with overwound ends as described by Garrett[6] supplied a uniform longitudinal magnetic field.

Four identical coils were housed in the sample holder, one of which remained empty while the other three contained a pure indium standard and two alloy specimens, respectively. Appropriate switching at room temperature connected the empty pickup coil in electrical opposition to any one of the other three coils and in series with a ballistic galvanometer. A signal proportional to the specimen's magnetic moment was produced when the applied magnetic field was removed. The ends of the samples extended beyond the ends of the pickup coils, thus permitting voltage and current leads to be attached. The critical field could thus be measured by noting the abrupt change in either the resistance or magnetic moment of a sample. Excellent agreement was found between the two techniques in the region of overlap. Magnetization measurements were favored near $T_c$, where the critical fields are small, to avoid the extraneous effects of the finite measuring current. At low temperatures, however, where the critical fields were large, the magnetization measurements were unsuitable because of the large transients produced when the external field was turned off.

### III. Results and Discussion

In Fig. 1 is shown the variation with composition of the residual resistance ratio $\Gamma=R_{4.2}/(R_{273}-R_{4.2})$, where $R_{4.2}$ is the measured resistance at 4.2°K and $R_{273}$ is the measured resistance at 273°K. In this plot are shown the compositions determined in two ways: first, those calculated from the weights of the melt constituents from which the specimens were fabricated; second, those determined from chemical analysis of the samples. The smooth curve was determined by a least-square fit of $\Gamma=ac-bc^2$ to the data, where $c$ is the tin concentration in atomic percent. The values determined for $a$ and $b$ are, respectively, $4.31\times10^{-2}$ and $1.26\times10^{-3}$. If one assumes that the "intrinsic" resistivity of the alloy, $\rho_{273}-\rho_{4.2}$, is the same as that measured by White and Woods[7] for indium, 7.97 $\mu\Omega$ cm, then one can calculate the residual resistivities of the alloys from $\Gamma$. For 1% Sn, one calculates a residual resistivity, $\rho_{4.2}$, of 0.33 $\mu\Omega$ cm, which agrees within about 6% with the data reported by Chanin *et al.*[8] In the second portion of this paper, the residual resistivities of the bulk alloys will be compared to the intrinsic residual resistivities of the alloy films.

Figure 2 shows the composition dependence of critical temperature, showing the characteristic minimum. For

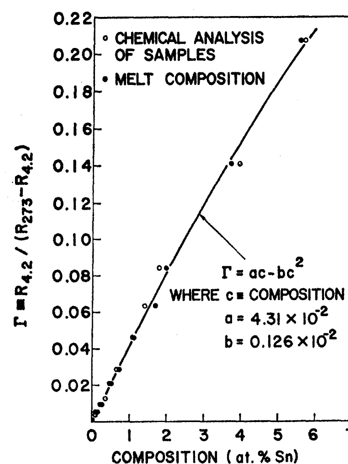


FIG. 1. The variation of residual resistivity ratio $\Gamma$ with composition. The solid curve shown was obtained by a least-squares fit to the data.

[2] A. M. Toxen, Phys. Rev. **124**, 1018 (1961).
[3] A. M. Toxen, Phys. Rev. **127**, 382 (1962).
[4] A. M. Toxen and M. J. Burns, Phys. Rev. **130**, 1808 (1963).
[5] A. M. Toxen, Rev. Mod. Phys. **36**, 308 (1964).
[6] M. W. Garrett, J. Appl. Phys. 22, 1091 (1951).
[7] G. K. White and S. B. Woods, Rev. Sci. Instr. **28**, 638 (1957).
[8] G. Chanin, E. A. Lynton, and B. Serin, Phys. Rev. **114**, 719 (1959).

comparison, we include the results of Merriam and von Herzen[9] which agree well.

Because of broadening of the critical-field transition at low temperatures for the high concentration samples, critical-field data were taken only near $T_c$ for the samples containing more than 2.4 at.% Sn. The critical-field slope at $T_c$, $(dH_c/dT)_{T_c}$, was calculated from the critical-field data and is plotted in Fig. 3.

In Fig. 4 is plotted the critical field at $T=0°K$, $H_0$. This was calculated by fitting to the $H_c$ versus $T$ data an analytical curve of the form $H_c=H_0+C_1T^2+C_2T^3$ in the manner described by Reeber.[10]

A useful description of the behavior of the critical-field–temperature relation under the variation of some independent parameter such as composition, stress, or isotopic mass (for which the concept was introduced) is given by assumption of the so-called similarity conditions.[11]

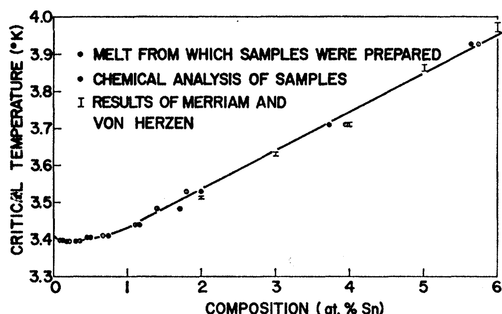


FIG. 2. The variation of critical temperature with composition.

The first similarity condition states that the entire family of reduced critical-field curves can be represented by a single function $F(t)$ whose form does not depend upon the value of the independent variable, i.e.,

$$H_c(t,X)/H_0(X)=F(t)\,, \qquad (1)$$

and

$$F(0)\equiv 1\,, \quad F(1)\equiv 0\,,$$

where $t$ is the reduced temperature $T/T_c(X)$, and $X$ is an independent variable. The second similarity condition is that

$$H_0(X)/T_c(X)=H_0(0)/T_c(0)\,. \qquad (2)$$

In Fig. 5 are shown critical-field data for indium-tin alloy specimens containing up to 1.81 at.% Sn. For comparison, the critical-field data of Shaw, Mapother, and Hopkins[12] for pure indium are included. The agreement between the various sets of data is good, being within ±1% or less for most of the data points shown. Thus similarity condition (1) is satisfied quite well by the dilute specimens. There is a further quantitative

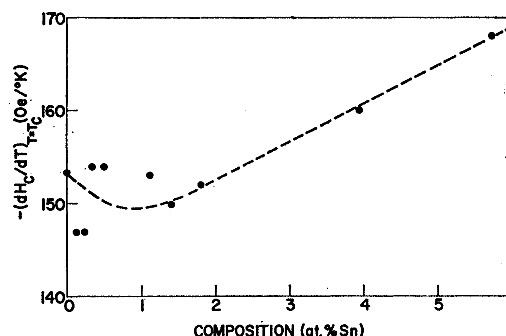


FIG. 3. The variation with composition of the critical-field slope at the critical temperature $-(dH_c/dT)_{T_c}$.

check on relation (1), for if $F(t)$ is to be independent of composition, then $F'(1)=(T_c/H_0)(dH_c/dT)_{T_c}$ will be a constant. In Table I are summarized values of the

TABLE I. Verification of the similarity of the bulk critical-field curves.[a]

| Sample composition (at.% Sn) | $T_c$ (°K) | $H_0$ (Oe) | $-(dH_c/dT)_{T_c}$ (Oe/°K) | $H_0/T_c$ (Oe/°K) | $-(T_c/H_0)(dH_c/dT)_{T_c}$ |
|---|---|---|---|---|---|
| 0.00[b] | 3.408 | 285.7 | 153.4 | 83.8 | 1.83 |
| 0.12 | 3.397 | 281.3 | 147 | 82.8 | 1.78 |
| 0.22 | 3.395 | 281.1 | 147 | 82.8 | 1.78 |
| 0.34 | 3.396 | 283.4 | 154 | 83.5 | 1.85 |
| 0.49 | 3.406 | 284.6 | 154 | 83.6 | 1.84 |
| 0.67 | 3.411 | 282.4 | 151 | 82.8 | 1.82 |
| 1.11 | 3.441 | 287.6 | 153 | 83.6 | 1.83 |
| 1.41 | 3.484 | 293.5 | 150 | 84.2 | 1.78 |
| 1.81 | 3.530 | 298.2 | 152 | 84.5 | 1.80 |

[a] See Part 1, Sec. III of text.
[b] See Ref. 12.

quantities $T_c$, $H_0$, $(dH_c/dT)_{T_c}$, and $F'(1)$. The values of $F'(1)$ are indeed nearly constant and are in good agreement with the value −1.82 predicted by the BCS theory.[13] One can also use the constancy of $F'(1)$ to calculate $H_0$ from $(dH_c/dT)_{T_c}$. These results are shown in Fig. 4. The values of $H_0/T_c$ are also nearly constant.

This similarity of the critical-field curves makes it very convenient when one wishes to calculate $H_c(X,T)$, i.e., the critical field for any composition $X$ and temperature $T$. For any sample of known composition, one

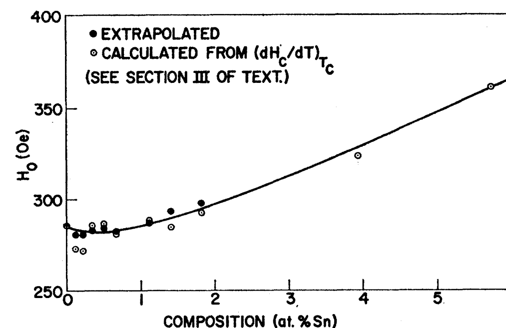


FIG. 4. The variation with composition of the critical field at 0°K.

[9] M. F. Merriam and M. von Herzen, Phys. Rev. **131**, 637 (1963).
[10] Morton D. Reeber, Phys. Rev. **117**, 1476 (1960).
[11] M. Garfinkel and D. E. Mapother, Phys. Rev. **122**, 459 (1961).
[12] R. W. Shaw, D. E. Mapother, and D. C. Hopkins, Phys. Rev. **120**, 88 (1960).
[13] J. Bardeen, L. N. Cooper, and J. R. Schrieffer, Phys. Rev. **108**, 1175 (1957).

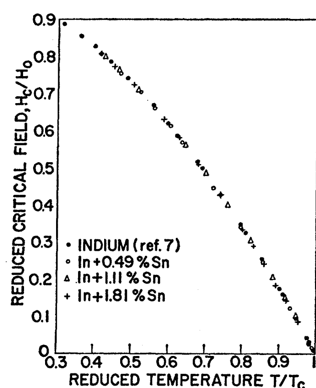


FIG. 5. A comparison of the reduced critical-field curves of indium-tin alloys to that of pure indium.

can obtain from Figs. 2 and 4 values for $T_c$ and $H_0$. One then calculates the reduced temperature $T/T_c$ corresponding to the temperature $T$. From Fig. 5, $H_c/H_0$ is obtained and then $H_c(X,T)$ is calculated.

## PART 2: FILMS

## I. Preparation of Films

### *Vacuum System*

The films used in this study were produced by evaporation from a single source onto fused quartz substrates positioned at a distance of approximately 17 cm from the melt surface.

A diagram (roughly to scale) of the vacuum system and evaporation chamber is shown in Fig. 6. Provision is made for a high-temperature vacuum "bake-out" of the entire evaporation chamber for the purpose of attaining lower system pressures, and, in particular, to aid in removing absorbed water vapor. Further, since the "gettering" ability of In and Sn is rather poor for most residual gases, a titanium vapor pump,[14] which continuously evaporates titanium from a hot-wire filament onto the walls of the pump, is incorporated into the system to provide for additional "gettering" and thus enable us to achieve lower ultimate system pressures. With this system and the baking and outgassing procedure to be described below we were able to achieve pressures (prior to evaporation) as low as $2.0\times10^{-10}$ mm Hg. System pressures were measured with a W.R.W. Electron Corporation type WR-75 ionization gauge. During evaporation, the system pressure was generally of the order of $10^{-7}$ mm Hg.

In order to obtain reproducible measurements, it was necessary to avoid highly agglomerated films. This was accomplished by maintaining the substrates in good thermal contact with a liquid-nitrogen reservoir during evaporation, a procedure which has the additional advantage of providing a constant, reproducible substrate temperature.

### *Basic Melts*

The evaporation charges were prepared by inserting carefully weighed amounts of high-purity (99.999%) In and Sn into a previously degassed cylindrical tantalum crucible. Both solute and solvent material were cut from 0.030-in.-diam Tadanac Brand H.P. wire. In order to maintain the source-to-substrate distance constant the total charge weight was approximately equal for all evaporations, and only the relative amounts of solute and solvent material were changed to vary the melt composition.

### *Substrates*

The substrates used were ground and polished fused quartz plates[15]—(5/8×7/16×0.040 in.). Since substrate cleanliness is an important factor in reproducibly evaporating films, the substrates were cleaned thoroughly prior to evaporation by washing in a hot detergent solution, followed by a one-hour soaking in hot chromic acid and a thorough rinsing in distilled water. Additional cleaning and removal of absorbed water vapor were provided during the high-temperature vacuum "bake-out" of the evaporation chamber.

### *"Bake-Out" and Degassing of Charge*

The tantalum crucible, containing the evaporation charge, was sealed into the evaporation chamber, and the assembly "baked out" at 300°C for approximately sixteen hours. Upon completion of the "bake-out," the oven was removed and the charge heated to 730°C by induction heating and degassed at this temperature for approximately 8 h. This "bake-out" and degassing cycle was then repeated a second time, after which the charge was evaporated as described below. A magnetically controlled shutter was used to shield the substrates during the melt degassing when a small portion of the charge was evaporated.

### *Evaporation*

After completion of the outgassing cycle, the charge temperature was increased slowly to a value about

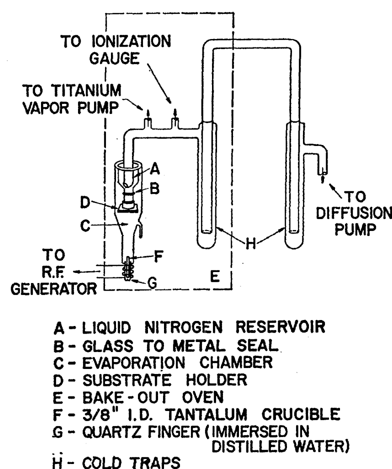


FIG. 6. Diagram of the vacuum system and evaporation chamber (roughly to scale).

[14] Obtained from Vacuum Instrument Corporation, Huntington Station, New York.

[15] Obtained from the Thermal American Fused Quartz Company, Dover, New Jersey.

10°C in excess of the desired evaporation temperature (which for this work varied from 1150 to 1210°C) and maintained for a few seconds. The temperature was then reduced to the desired value, the masking shutter opened for a predetermined time, and a portion of the melt was evaporated. This procedure of exceeding the evaporation temperature for a few seconds and evaporating a portion of the melt prior to producing the samples served to eliminate, or at least to minimize, the surface slag present when the melt contained an appreciable concentration of tin. This slag not only tends to enhance melt spattering but also produces fluctuations in the evaporation rate. After evaporation, the films were removed from the evaporation chamber, and a four-terminal network pattern for resistance measurements was trimmed from the film. Although the edges of a trimmed film are rougher than those of a film evaporated through a mask, the trimming serves to remove the edge regions of the films. This is desirable since the edges, being thinner than the remaining bulk of the film, have a higher critical field than the film proper and thus tend to produce excessive broadening of the resistive transition.

## II. Experimental Results on Films

### *A. Film Composition*

Although it is quite feasible to control the Sn content of evaporated In-Sn alloy films to within ±0.2 at.% Sn by evaporating to completion a single In-Sn source,[16] a considerable amount of melt spattering takes place which produces a somewhat irregular film surface. It was for this reason that the films reported on in this paper were produced by the evaporation of only a small fraction of the total alloy melt. Because of the relatively large difference in the vapor pressures of indium and tin, the In evaporation rate is much higher than that of Sn and consequently the Sn content of films produced by this technique differed considerably from that of the crucible melts. The composition could, however, be varied over the desired range (0 to 5 at.% Sn) by adjusting the melt compositions and the evaporation temperatures and times. Figure 7 shows the dependence of film deposition rate upon the melt composition for a group of In-Sn alloy films evaporated at 1165°C. The deposition rates shown varied from about 100 Å/sec to slightly over 800 Å/sec.

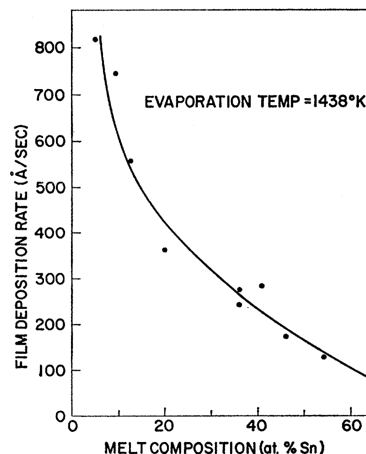


FIG. 7. The dependence of film deposition rate upon melt composition for a group of films evaporated at about 1165°C.

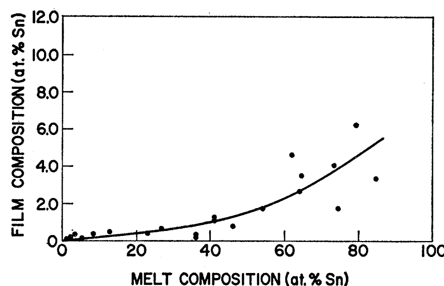


FIG. 8. The dependence of film composition upon melt composition for films evaporated at approximately 1165°C.

In Fig. 8 is shown the dependence of film composition upon melt composition. The compositions of the In-Sn films were measured by Miksic[17] using an x-ray fluorescence technique capable of determining the Sn content of these films to ±0.05 at.% Sn. Variation in the film composition was minimized by evaporating only a fraction of the melt. Since we evaporated the films from a single source, rather than simultaneously depositing the two constituents from independent sources, composition variation over the area of the film was eliminated. There may have existed some initial composition variation throughout the film thickness. But, since the resistive transitions of the films are quite sharp, we believe this variation to have been eliminated by diffusion at room temperature.

### *B. Critical-Field Measurements*

The critical fields of the films were measured in the same manner as that previously reported for pure indium films.[1] In essence, the critical field is determined by noting that tangential field at which the resistance of the film appears. In all but the highest concentration films, the resistance transitions are quite sharp and are independent of the measuring current (provided that the measuring current is well below the critical current).

In Fig. 9 is shown the effect of varying Sn content upon the critical field curves for a group of In-Sn alloy films of comparable thickness. Because the critical-field data have been analyzed and reported elsewhere,[3-5] we will not discuss them further in this communication.

### *C. Electrical Properties*

From measurements of the room temperature resistance $R_{295}$ and residual resistance $R_0$, we can, by making a few reasonable assumptions, calculate for each film its thickness $d$ and residual resistivity $\rho(0)$. First,

[16] M. J. Burns and M. G. Miksic (unpublished data).

[17] M. G. Miksic (private communication).

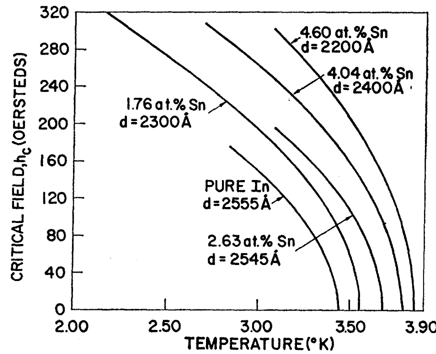


FIG. 9. The variation of critical field with temperature for a group of films having approximately the same thickness, but different compositions.

assuming the room-temperature resistivity to be the sum of the residual (or temperature-independent) resistivity and the intrinsic resistivities, we obtain for the residual resistivity the expression

$$\rho(0)=\rho_i(295)R_0/(R_{295}-R_0)\,, \tag{3}$$

where $\rho_i(295)$ is the intrinsic resistivity at 295°K (room temperature). We shall assume that $\rho_i(295)$ is the same in the dilute indium-tin alloys as it is for pure indium and will use the value of $\rho_i(295)=8.8\ \mu\Omega$ cm obtained by White and Woods.[7] Using the same assumptions as above, we can determine the following expression for the film thickness:

$$d=\rho_i(295)L/W(R_{295}-R_0)\,, \tag{4}$$

where $L$ is the film length, and $W$ is its width.

The residual resistances of the films will have two contributions, scattering at the film boundaries and scattering from defects distributed throughout the "volume" of the film such as tin atoms in the indium matrix. To separate these contributions, one must utilize a theoretical model for the boundary scattering. For this purpose one may use Fuchs' model[18] which agrees reasonably well with resistivity-versus-size measurements of indium foils,[19] wires,[20] and evaporated films.[1] Fuchs' model is ordinarily given in the following form:

$$\frac{\rho}{\rho_0}=\left[1-\frac{3k}{4}\left(1-\frac{k^2}{12}\right)E_i(-k)-\frac{3}{8k}(1-e^{-k})-\left(\frac{5}{8}+\frac{k}{16}-\frac{k^2}{16}\right)e^{-k}\right]^{-1}, \tag{5}$$

where $\rho$ is the measured resistivity (including boundary scattering), $\rho_0$ is the "intrinsic" resistivity, i.e., the resistivity in the absence of boundary scattering, $k$ is the ratio of the thickness $d$ to the intrinsic mean free path $l_0$, and $E_i(-k)$ is the exponential integral.[21] Thus, we see that the above expression is of the form

$$\rho/\rho_0=F(d/l_0)\,. \tag{6}$$

For our purposes this expression is not too convenient, for we know $\rho$ and $d$ and wish to calculate $\rho_0$ and $l_0$. Since the product of resistivity and mean free path, $\rho_0 l_0$, is, for a given material, a constant,[22] i.e.,

$$\rho_0 l_0=A\,, \tag{7}$$

we can solve Eqs. (6) and (7) simultaneously for $\rho_0$ and $l_0$ if we know the value of $A$. There is, however, a more convenient way of calculating $\rho_0$ and $l_0$. Let us multiply both sides of Eq. (5) by $d/l_0$. We then obtain

$$y=\left[\frac{1}{k}-\frac{3}{4}\left(1-\frac{k^2}{12}\right)E_i(-k)-\frac{3}{8k^2}(1-e^{-k})-\left(\frac{5}{8}+\frac{k}{16}-\frac{k^2}{16}\right)\frac{e^{-k}}{k}\right]^{-1}, \tag{8}$$

where $y=\rho d/A$. We can then solve Eq. (8) to find $k(y)$. This is plotted in Fig. 10 and for the benefit of the reader is tabulated in Table II. One could equally well calculate $\rho_0/\rho$ as a function of $y$, since $k=y\rho_0/\rho$. Once we have solved (8) for $k$ in terms of $y$, we have a truly useful relation. For $\rho$ and $d$ are directly measurable quantities and $A$ is determined from measurements of $\rho$ versus $d$ for any material. Hence, we can calculate $y=\rho d/A$. Then

$$l_0=d/k(y)\,, \tag{9}$$

and

$$\rho_0=Ak(y)/d. \tag{10}$$

Thus we see that $l_0$ and $\rho_0$ are both monotonic functions of the quantity $y$. In Fig. 11 are plotted the values for $\rho_0$ calculated for the indium-tin alloy films from Eq. (10) with $\rho$ and $d$ determined by means of Eqs. (3) and (4), and $A=2.0\times10^{-11}\ \Omega\text{cm}^2$, a value determined from measurements on pure indium films.[1] The solid curve is the residual resistivity of the bulk alloys

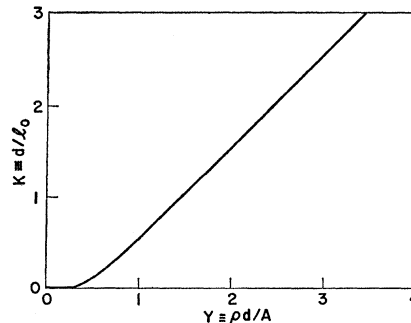


FIG. 10. The dependence of intrinsic mean free path upon thickness and measured resistivity. The plot shown is of Eq. (8) of the text using the data of Table II.

[18] K. Fuchs, Proc. Cambridge Phil. Soc. **34**, 100 (1938).
[19] A. Gaide and P. Wyder, Helv. Phys. Acta (to be published).
[20] J. F. Olsen, Helv. Phys. Acta **31**, 713 (1958).
[21] E. Jahnke and F. Emde, *Tables of Functions* (Dover Publications, New York, 1945), p. 1.
[22] See for example D. K. C. MacDonald, *Encyclopedia of Physics*, edited by S. Flügge (Springer-Verlag, Berlin, 1956), Vol. XIV, p. 188.

TABLE II. Modification of Fuchs' formula to directly calculate intrinsic resistivity or mean free path from measured resistivity and thickness.

| $k\equiv d/l_0$ | $y\equiv\rho d/\text{Å}$ | $k\equiv d/l_0$ | $y\equiv\rho d/\text{Å}$ | $k\equiv d/l_0$ | $y\equiv\rho d/\text{Å}$ |
|---|---|---|---|---|---|
| 0.02 | 0.3064 | 0.80 | 1.2637 | 2.10 | 2.5400 |
| 0.05 | 0.3870 | 0.85 | 1.3135 | 2.20 | 2.6385 |
| 0.10 | 0.4784 | 0.90 | 1.3633 | 2.30 | 2.7367 |
| 0.15 | 0.5527 | 0.95 | 1.4130 | 2.40 | 2.8345 |
| 0.20 | 0.6192 | 1.00 | 1.4620 | 2.50 | 2.9317 |
| 0.25 | 0.6809 | 1.05 | 1.5115 | 2.60 | 3.0303 |
| 0.30 | 0.7397 | 1.10 | 1.5605 | 2.70 | 3.1279 |
| 0.35 | 0.7964 | 1.20 | 1.6592 | 2.80 | 3.2268 |
| 0.40 | 0.8512 | 1.30 | 1.7568 | 2.90 | 3.3256 |
| 0.45 | 0.9052 | 1.40 | 1.8549 | 3.00 | 3.4258 |
| 0.50 | 0.9579 | 1.50 | 1.9527 | 3.20 | 3.6219 |
| 0.55 | 1.0102 | 1.60 | 2.0504 | 3.40 | 3.8182 |
| 0.60 | 1.0617 | 1.70 | 2.1487 | 3.60 | 4.0161 |
| 0.65 | 1.1127 | 1.80 | 2.2457 | 3.80 | 4.2141 |
| 0.70 | 1.1633 | 1.90 | 2.3441 | 4.00 | 4.4111 |
| 0.75 | 1.2142 | 2.00 | 2.4414 | | |

and was calculated from the solid curve of Fig. 1 assuming that the ideal resistivity at 273°K is $7.97\mu\ \Omega$cm, the value for pure indium. Except for the most dilute films, the intrinsic residual resistivities of the films are slightly less than the residual resistivity of the bulk samples. For those samples containing more than 2 at.% Sn, the difference is about 10%. In the case of the more dilute films, there is too much scatter in the data to draw any inferences other than the observation that the intrinsic film resistivities are roughly the same as the bulk residual resistivities. The large amount of scatter in the dilute film data is undoubtedly due to the large correction which must be made for boundary scattering since $\rho_0/\rho\sim 0.1$ for the dilute films. Had we chosen a slightly smaller value for $A$, viz. $1.6\times 10^{-11}\ \Omega\text{cm}^2$, the intrinsic resistivities of the more concentrated films (that is, those containing more than 2 at.% Sn) would have been in almost exact agreement with the bulk residual resistivities.

Thus we see that the use of a value for $\rho l$ of approximately $2\times 10^{-11}\ \Omega\text{cm}^2$ leads to values of the intrinsic residual resistivity of the indium-tin alloy films in very

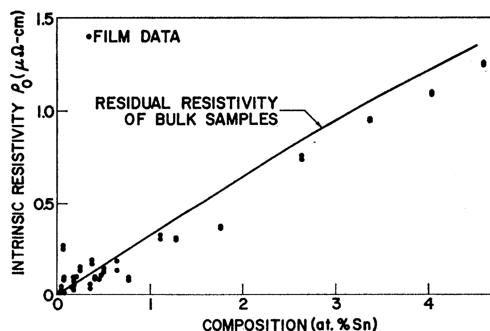


FIG. 11. The variation of intrinsic resistivity $\rho_0$ with composition for the alloy films. The solid curve is the residual resistivity of the bulk alloys and was obtained from the solid curve of Fig. 1. The dots are the film results calculated from the measured thicknesses and resistivities using Fuchs' model as discussed in Part 2, Sec. IIC of the text.

good agreement with the measured residual resistivity of the bulk alloys of the same composition. Or one might turn the argument around and ask what value for $\rho l$ gives values for the film intrinsic residual resistivities in agreement with the measured bulk residual resistivities. From this point of view one could infer $\rho l\simeq 1.6\times 10^{-11}\ \Omega\text{cm}^2$ for the dilute indium-tin alloys. It has also been found[4] that the superconducting properties of these indium-tin films (in particular the critical fields) are consistent with a value for $\rho l$ of $1.6\text{–}2.0\times 10^{-11}\ \Omega\text{cm}^2$. It is quite significant that the value for $\rho l$ inferred from the measurements on the alloy films agrees quite well with those values deduced from measurements on pure indium samples: $2.0\times 10^{-11}\ \Omega\text{cm}^2$ for indium films,[1] $1.6\times 10^{-11}\ \Omega\text{cm}^2$ for indium foils,[19] and $1.8\times 10^{-11}\ \Omega\text{cm}^2$ for wires.[20] Thus all of the above values for $\rho l$ which have been determined from dc measurements are consistent with one another but disagree by a factor of 3 with the value for $\rho l$ of $0.57\times 10^{-11}\ \Omega\text{cm}^2$ deduced by Dheer[23] from high-frequency surface impedance measurements. It is felt that this discrepancy is real and is a result of large variations in mean free path for carriers associated with different regions of the Fermi surface. It has been pointed out by Bate, Martin, and Hille,[24] that while the bulk dc conductivity depends upon the average value of the mean free path, $\langle l\rangle$, the dc conductivity of a specimen in the presence of boundary scattering depends upon the average value of the square of the mean free path $\langle l^2\rangle$ as well. Since $\langle l^2\rangle$ is always greater than or equal to $\langle l\rangle$,[2] the value of $\rho l$ obtained from dc size effect measurements should be larger than that obtained from anomalous skin-effect measurements. Thus one can reconcile the dc and high-frequency results if there is a large variation of $l$ over the Fermi surface. This point will be pursued in a future publication.

### *D. Critical Temperature*

The critical temperatures of the films were obtained most conveniently by extrapolation of the $H_c$ versus $T$ data to obtain that temperature at which $H_c=0$. In Fig. 12 are shown the measured values of $T_c$ for the films together with the curve for the bulk alloys shown in Fig. 2. It is clear from Fig. 12 that the critical temperatures of the films are, in general, higher than those of the corresponding bulk specimens. This was previously observed to be the case for pure indium films,[1] where it was concluded that the shift in $T_c$ was a stress effect caused by differential contraction of film and substrate on being cooled to low temperatures. It was further concluded that the stresses were great enough to cause plastic flow in the films. Hence, the shift in critical temperature is a measure of the yield stress of the films. For the pure indium films, it was found that the shift

[23] P. N. Dheer, Proc. Roy. Soc. (London) **A260**, 333 (1961).
[24] R. T. Bate, Byron Martin, and P. F. Hille, Phys. Rev. **131**, 1482 (1963).

in critical temperature was inversely proportional to the film thickness. A least-squares fit to the data gave the result

$$\delta T_c = 51.4/d, \tag{11}$$

where $d$ is the thickness in Å, and $\delta T_c$ is the temperature shift in degrees Kelvin. In the alloy films, one would expect to find, in addition to the thickness effects, composition effects such as alloy hardening,[25] etc. To separate the composition effects from the thickness effects we shall make the assumption that the two effects are additive. In Fig. 13 we have plotted $\Delta T_c = T_c^{\text{film}} - T_c^{\text{bulk}} - \delta T_c(d)$ as a function of film composition, where $\delta T_c(d)$ is calculated from Eq. (11). For low tin concentrations, $\Delta T_c$ increases linearly with tin content. This is in accord with the simple theories of solid solution hardening.[25] However, for tin concentrations greater than about 1%, $\Delta T_c$ ceases to increase with increasing tin concentration. In fact, $\Delta T_c$ reaches a maximum and then starts decreasing with further increase in tin concentration. The result is well outside of any reasonable estimate of the experimental errors. The values for $T_c^{\text{film}}$ and $T_c^{\text{bulk}}$ are estimated to be accurate to $\pm 0.005$°K or less. Because all of the films are fairly thick, i.e., $\gtrsim 2000$ Å, the thickness correction $\delta T_c$ is not large, being 0.010–0.023°K for almost all of the data shown. Hence, the assumption of additivity of thickness and composition effects cannot introduce a very large error. Certainly this error is less than $\delta T_c$ itself. Uncertainties in the composition of the bulk or film sample should introduce error in $\Delta T_c$ of no more than $\pm 0.020$°K. To make the points at 4% Sn and 4.6% Sn lie on a straight line through the dilute alloy data would require an error in $\Delta T_c$ of about 0.150°K which is about an order of magnitude greater than the estimated errors.

It is not at all certain what the explanation of this behavior is, since the lattice parameters hardly change over the composition range in question. According to Fink *et al.*,[26] $a$ changes by $-0.3\%$ and $c$ by $+1.0\%$ over the composition range 0–4.7% Sn. One possible explanation is afforded by the phenomenon of twinning, which can relieve stresses, but does not involve the ordinary dislocation motion characteristic of slip. It is well known that indium twins. Hence, this mechanism can provide an upper limit to the stress that the films can sustain and will explain the "leveling off" of $\Delta T_c$ for concentrations of tin greater than 1%. In the most dilute specimens, slip dominates and we see the increase in $\Delta T_c$ characteristic of alloy hardening. When the stresses in the films become large enough to cause twinning, this mechanism becomes dominant, and $\Delta T_c$ fails to increase with increasing tin concentration. Further, it is known that in certain metals, such as Mg, Ge, Cd, and $\alpha$-Fe, impurities actually facilitate the formation of twin bands.[27] If the addition of tin facilitates twinning in the films, then the more concentrated alloy films could have a yield stress lower than that of the more dilute films and $\Delta T_c$ for the former could actually decrease with increasing tin content.

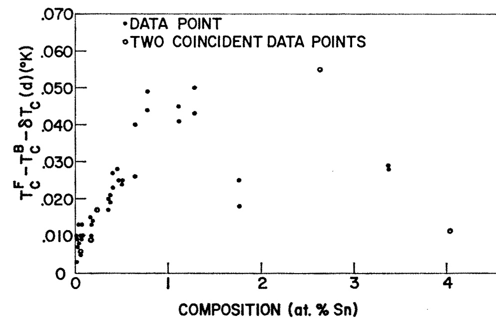


FIG. 13. Difference between film and bulk critical temperatures due to alloy hardening. The data shown are obtained by subtracting from the film critical temperature the bulk critical temperature and the size-dependent critical temperature shift measured on pure indium films (see Part 2, Sec. IID of the text).

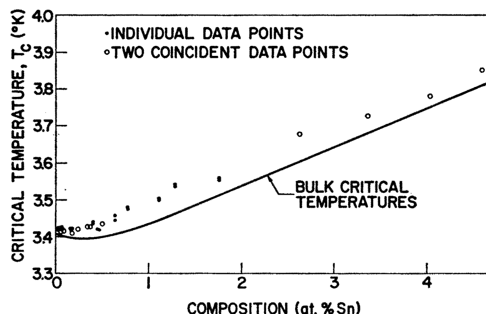


FIG. 12. Variation of critical temperature with composition. The solid curve represents the bulk data (see Fig. 2). The dots are the alloy film data.

## III. Stress Modification of Critical Field

In the theoretical models describing the critical fields of thin films,[3–5] the quantity which is of interest is the ratio of the critical field of the film to the critical field of a bulk sample of the same material and at the same temperature. Because the critical temperatures of the films are different from those of bulk samples having the same composition, this presents a problem. The problem can be resolved, however, by calculating the critical field of a bulk specimen which is subjected to the same system of stresses as those imposed upon the films.

The stress-shifted critical field $H_c'$ will be given approximately by the expression

$$H_c'(T) = H_c(T) + \sum_i (\partial H_c/\partial\sigma_i)\sigma_i, \tag{12}$$

where $H_c(T)$ is the critical field at zero stress, $\sigma_i$ are the applied uniaxial stresses, and where we drop higher-order terms in the Taylor series expansion of $H_c'$. We

[25] A. H. Cottrell, *Dislocations and Plastic Flow in Crystals* (Oxford University Press, London, 1958), p. 125 ff.

[26] C. G. Fink, E. R. Jette, S. Katz, and F. J. Schnettler, Trans. Electrochem. Soc. **88**, 229 (1945).

[27] R. Clark and G. B. Craig, Progr. Metal Phys. **3**, 121 (1952).

then evaluate the second term in the right-hand side of (12) by imposing the same system of stresses as those to which the films are subject. This is done as follows: If one applies a uniaxial stress $\sigma$ to a tetragonal crystal, then[28]

$$\partial H_c/\partial\sigma = (\partial H_c/\partial\sigma_p)\cos^2\theta + (\partial H_c/\partial\sigma_s)\sin^2\theta\,, \quad (13)$$

where $\sigma_p$ is the stress component parallel to the tetragonal axis, $\sigma_s$ is the stress component perpendicular to the tetragonal axis, and $\theta$ is the angle which $\sigma$ makes with the tetragonal axis. From the stress measurements of Rohrer[29] on indium,

$$\begin{aligned}\partial H_c(t)/\partial\sigma_p &= (3.4+2.8t^2)\times10^{-9}\text{ Oe cm}^2/\text{dyn}\\ \partial H_c(t)/\partial\sigma_s &= (0.2+0.1t^2)\times10^{-9}\text{ Oe cm}^2/\text{dyn}\,,\end{aligned} \quad (14)$$

where $t=T/T_c{}^B$. X-ray measurements[30] made on the indium-tin (and pure indium) films indicate that the films all have a strong preferred orientation with the (111) planes of the face-centered tetragonal cells parallel to the substrate surface. At liquid-helium temperatures,[31] the $c/a$ ratio in indium is 1.08. Hence one can resolve the biaxial stress in the plane of the substrate into equal normal uniaxial components making angles of 37°22′ and 90° with the $c$ axes of the grains. From Eqs. (12)–(14), one finds that

$$H_c{}'(T) = H_c(T) + K(T)\sigma\,, \quad (15)$$

where $k(T)=2.41[1+0.79(T/T_c{}^B)^2]\times10^{-9}$ Oe cm²/dyn, and $\sigma$ is the magnitude of the uniaxial stress components. If one now makes the assumption that the shift in critical temperature of the films is due entirely to the stresses induced by the differential contraction of substrate and film upon cooling from room temperature, then the quantity $\sigma$ in (15) can be easily evaluated, since $H_c{}'(T_c{}^F)=0$. Because $T_c{}^F-T_c{}^B$ will be small for all of the films under consideration, it will be sufficiently accurate to assume that $H_c(T)$ is linear over the interval $T_c{}^B<T<T_c{}^F$, i.e., that

$$H_c(T)\simeq(dH_c/dT)_{T_c{}^B}(T-T_c{}^B) \quad \text{for} \quad T_c{}^B<T<T_c{}^F. \quad (16)$$

One then obtains from (15) and (16) the desired result for $\sigma$,

$$\sigma\simeq|dH_c/dT|_{T_c{}^B}(T_c{}^F-T_c{}^B)/k(T_c{}^F)\,. \quad (17)$$

By substituting (17) into (15), one obtains the general expression for the stress-shifted bulk critical field,

$$H_c{}'(T)=H_c(T)+|dH_c/dT|_{T_c{}^B}\times(T_c{}^F-T_c{}^B)k(T)/k(T_c{}^F)\,, \quad (18)$$

where $H_c(T)$ is the measured unshifted bulk critical field for $T<T_c{}^B$, but is approximated by (16) for $T_c{}^B<T<T_c{}^F$.

It is easy to see from (18) how well the similarity condition $H_c{}'(0)/T_c{}^F=H_c(0)/T_c{}^B$ is obeyed. Let

$$|dH_c/dT|_{T_c{}^B}\equiv DH_c(0)/T_c{}^B\,, \quad (19)$$

where $D$ is in general of the order of unity. In Part 1, Sec. III, it was pointed out that the BCS theory yields a value of 1.82 for $D$. Upon substitution of (19) into (18), one obtains for $T=0$ the result

$$H_c{}'(0)=H_c(0)+D[H_c(0)/T_c{}^B]\times(T_c{}^F-T_c{}^B)[k(0)/k(T_c{}^F)]\,. \quad (20)$$

If one adds and subtracts $H_0(T_c{}^F-T_c{}^B)/T_c{}^B$ to the right-hand side of (20) and divides the entire equation by $T_c{}^F$, one obtains after some manipulation the desired result:

$$\frac{H_c{}'(0)}{T_c{}^F}-\frac{H_0}{T_c{}^B}\left\{1+\frac{T_c{}^F-T_c{}^B}{T_c{}^F}\left(\frac{Dk(0)}{k(T_c{}^F)}-1\right)\right\}\,. \quad (21)$$

From (21), it is clear that the departure from this similarity condition is just proportional to the shift in critical temperature of the films from the bulk value. However, for the alloy films discussed in this paper, the quantity in the curly brackets of (21) is extremely close to unity. Since $T_c{}^F$ is no more than 2% larger than $T_c{}^B$ for the films considered here, $(T_c{}^F-T_c{}^B)/T_c{}^F\leq0.02$. Even more significantly, for these films $k(T_c{}^F)/k(0)\simeq1.8$. But as Table I indicates, $D\simeq1.8$ for the dilute indium-tin alloys. Thus the quantity in parentheses in (21) is approximately zero for the films discussed. For other superconductors, this cancellation may not occur.

Consider next the other similarity condition, i.e., Eq. (1). If one divides (18) by (20) and substitutes for $|dH_c/dT|_{T_c{}^B}$ its value from (19), one obtains the following result:

$$\frac{H_c{}'(T)}{H_c{}'(0)}=\left[\frac{H_c(T)}{H_c(0)}+\left(\frac{T_c{}^F-T_c{}^B}{T_c{}^B}\right)\frac{Dk(T)}{k(T_c{}^F)}\right]\times\left\{1+\left(\frac{T_c{}^F-T_c{}^B}{T_c{}^B}\right)\frac{Dk(0)}{k(T_c{}^F)}\right\}^{-1}\,. \quad (22)$$

To save space, the following shorthand notation will be useful: $H_c{}'(T)/H_c{}'(0)\equiv F$, $H_c(T)/H_c(0)\equiv f$, $(T_c{}^F-T_c{}^B)/T_c{}^B\equiv\Delta$, $T/T_c{}^B\equiv t$, and $T/T_c{}^F\equiv t'$. In this notation, the similarity condition of Eq. (1) can be written as

$$F(t')=f(t)\,. \quad (23)$$

To see how well (23) is satisfied, one can expand $F(t')$ in a Taylor's series about $t$. To simplify the results, it is assumed that $\Delta\ll1$ so that all terms can be expanded in powers of $\Delta$. For the films considered in this paper $\Delta\leq0.02$, so this assumption is certainly justified. The

[28] D. P. Seraphim and P. M. Marcus, IBM J. Res. Develop. **6**, 94 (1962).
[29] H. Rohrer, Phil. Mag. **4**, 1207 (1959).
[30] R. Crosby (private communication).
[31] J. Graham, A. Moore, and G. V. Raynor, J. Inst. Metals **85**, 86 (1955).

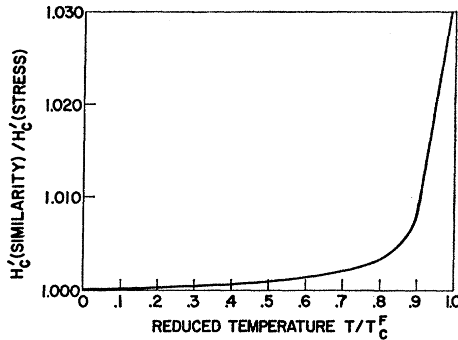


FIG. 14. A comparison of the stress-shifted bulk critical field calculated assuming similarity to that calculated from Eq. (18) of the text for a sample of In+2.6 at.% Sn.

result is that

$$F(t')=f(t)+\left[D\frac{k(t)}{k(T_c^F/T_c^B)} -tf'(t)-\frac{Dk(0)f(t)}{k(T_c^F/T_c^B)}\right]\Delta+O(\Delta^2). \quad (24)$$

Comparison of (24) to (23) indicates that the deviations from this similarity condition are just proportional to the magnitude of $\Delta$, as were the deviations from the other similarity condition as (21) indicated. Examination of the terms within the square brackets in (24) indicates that the coefficient of $\Delta$ vanishes at $t=0$ as it should, since $F(0)=f(0)=1$. From (15), the first term in the brackets is a monotonically increasing function of $t$. Since $f'(t)$ is negative, the second term is positive and is also an increasing function of $t$. The third term is negative and its magnitude decreases with increasing temperature. Therefore, the coefficient of $\Delta$ is an increasing function of $t$. Since $f(t)$ is a decreasing function of $t$, it is clear that the deviations from this similarity condition increase monotonically with $t$. These conclusions are borne out by detailed calculations. In Fig. 14 are shown calculations of the ratio of $H_c'(T)$, as calculated from (18), to $H_c'(T)$, calculated assuming similarity. These results are for a film of indium +2.6 at.% tin, for which $\Delta$ is greatest in value. As Fig. 14 indicates, the greatest deviation is about 3% and occurs at $t'=1$.

From Eq. (17) one can calculate the uniaxial stress $\sigma$ for any of the films. For In+2.6 at. % Sn, $\sigma$ is equal to $2.6\times10^9$ dyn/cm$^2$.

## SUMMARY AND CONCLUSIONS

Using a single source to obtain spatial homogeneity and cooled substrates to minimize agglomeration effects, high-purity alloy films of indium containing up to 5 at.% tin were prepared. The tin content of the films was measured to $\pm0.05$ at.% Sn using x-ray fluorescence techniques.

From resistance measurements, the critical temperatures, critical fields, thicknesses, and residual resistivities of the films were obtained.

The critical temperature measurements indicated that bulk and film specimens having the same composition did not have the same critical temperature. The most plausible explanation is that the films, which were rigidly attached to a substrate having a different coefficient of expansion, were in a stressed condition. On the basis of a model which attributed the entire shift in critical temperature to stress effects, formulas were derived which enabled one to calculate the equivalent (i.e., stress-shifted) bulk critical field for any film. However, the stress-shifted bulk critical field curves obtained in this way are nearly the same as one would have obtained under the assumption of similarity. Hence these corrected critical-field curves are not sensitive to the details of the stress model.

To calculate the intrinsic mean free path and intrinsic resistivity of the films more conveniently, Fuchs' formulas have been expressed in different form. In this form, the intrinsic mean free path and intrinsic resistivity can each be calculated directly from the measured resistivity and thickness.

From the analysis of the critical temperature and residual resistivity data, several interesting results were obtained. It appears that while stresses are relieved in the most dilute films by ordinary dislocation flow, some other mechanism, perhaps twinning, dominates in the more concentrated alloys. On the basis of the critical-temperature shift, it was estimated that the maximum uniaxial stress which could be sustained in the alloy films was $2.6\times10^9$ dyn/cm$^2$, which was calculated for a film of In+2.6 at.% Sn.

From the resistivity measurements, one may infer a value for $\rho l$ of $1.6\times10^{-11}$ $\Omega$cm$^2$, in excellent agreement with other results obtained by means of dc size effect measurements, but a factor of three larger than the result from anomalous skin effect measurements.

In addition to the indium-tin system, some work was done on indium-lead, indium-cadmium, indium-gallium, and indium-thallium films. In general, these materials were quite similar in their properties to the indium-tin alloys; however, a lack of time precluded more comprehensive studies.

## ACKNOWLEDGMENTS

We would like to express our appreciation to A. C. Burgess, R. E. Horstmann, and R. J. Parker for their help in carrying out these experiments and to Dr. D. P. Seraphim for his helpful advice and encouragement.